nature neuroscience

Gating and control of primary visual cortex by pulvinar

Gopathy Purushothaman[1], Roan Marion[2], Keji Li[3] & Vivien A Casagrande[1,3]

The primary visual cortex (V1) receives its driving input from the eyes via the lateral geniculate nucleus (LGN) of the thalamus. The lateral pulvinar nucleus of the thalamus also projects to V1, but this input is not well understood. We manipulated lateral pulvinar neural activity in prosimian primates and assessed the effect on supra-granular layers of V1 that project to higher visual cortex. Reversibly inactivating lateral pulvinar prevented supra-granular V1 neurons from responding to visual stimulation. Reversible, focal excitation of lateral pulvinar receptive fields increased the visual responses in coincident V1 receptive fields fourfold and shifted partially overlapping V1 receptive fields toward the center of excitation. V1 responses to regions surrounding the excited lateral pulvinar receptive fields were suppressed. LGN responses were unaffected by these lateral pulvinar manipulations. Excitation of lateral pulvinar after LGN lesion activated supra-granular layer V1 neurons. Thus, lateral pulvinar is able to powerfully control and gate information outflow from V1.

The primate visual system is currently viewed as a rough hierarchy of 30 or more cortical areas[1–4]. Area V1 is at the bottom of this hierarchy and contains a representation of important elementary visual features. Synaptic inputs from LGN, as well as intracortical circuits, are thought to underlie this important visual representation[1,2]. This model of visual system organization and function is incomplete in at least two aspects[4]. First, the model does not take into account the substantial input to V1 from pulvinar in elucidating V1 function[4–7]. Second, unlike cortico-cortical connections, cortico-pulvino-cortical projections are not hierarchical[4]. Lateral pulvinar receives input from infra-granular layer 5 of V1 and projects to supra-granular layers 1–3 of V1 as well as to layers 3–4 of the secondary visual area (V2)[5,8–10]. Supra-granular layers 2–3 of V1 also project to granular layer 4 of V2 (**Supplementary Fig. 1**)[5]. In addition to each subnucleus of pulvinar (for example, lateral pulvinar) projecting both forward and backward to multiple interconnected cortical areas (for example, V1 and V2), multiple subnuclei connect with the same cortical area[5]. In the absence of layers or columns in the subnuclei of pulvinar[5], this complex mesh of interconnections obscures the hierarchical position of pulvinar relative to V1 and V2 (ref. 4). Consequently, it is difficult to decipher the distinct function of each node along the cortico-pulvino-cortical pathway; it is also difficult to tease out the causal relationship between neural activity at different nodes[4,11].

Despite these complications, certain facts about the pulvinar nucleus make it necessary to address these two limitations. The pulvinar has expanded through evolution in proportion to the enlargement of higher visual and association cortices with which it connects[5–7]. Pulvinar lesions in monkeys and humans often result in profound visual deficits, such as spatial neglect and impaired attention[12–20]. Human and monkey experiments have shown pulvinar activity to be correlated with aspects of spatial vision, visual salience, attention and saccadic suppression[21–28]. Pulvinar atrophy is also characteristic of severe neuropsychiatric disorders and treatment of some of these disorders mitigates pathologies of the pulvinar[29]. That a single thalamic nucleus is associated with such a wide array of visual functions and causes such a variety of deficits when damaged is not easily explained. This motivates a better understanding of the position of pulvinar in the functional hierarchy of the visual system.

As a simple first step toward this goal, we studied the net effect of manipulating the activity of pulvinar neurons on their projection zone lowest in the cortical hierarchy, that is, the supra-granular layers of V1. We locally excited or suppressed neural activity in the lateral subnucleus of pulvinar and measured the effect of these manipulations on the V1 target zone of the affected lateral pulvinar neurons. For comparison and control, we also monitored and manipulated LGN neural activity in similar manner.

RESULTS

We measured the responses of neurons in superficial layers 2–3 of area V1 of *Otolemur garnettii* to high-contrast (50%) drifting sinusoidal gratings presented in the neurons' visual receptive fields (Online Methods and **Supplementary Fig. 2**). In each experiment, responses of multiple V1 neurons were simultaneously measured using a 100-electrode array implanted in one hemisphere. Receptive fields of neurons sampled by different electrodes of the array varied in size from 1° to 4° and were located within 6° of area centralis. These measurements revealed a characteristic brisk phasic response to onset of visual stimulation followed by a tonic response for the remainder of the stimulation (**Fig. 1a**).

Effect of reversible inactivation of lateral pulvinar

Using a microelectrode, we found lateral pulvinar neurons whose receptive fields overlapped with a majority of V1 receptive fields sampled by the array. Centrally located lateral pulvinar receptive fields that satisfied this criterion varied in size from 1° to 6° and were

[1]Department of Cell and Developmental Biology, Vanderbilt University, Nashville, Tennessee, USA. [2]Neuroscience Graduate Program, Vanderbilt University, Nashville, Tennessee, USA. [3]Department of Psychology, Vanderbilt University, Nashville, Tennessee, USA. Correspondence should be addressed to V.A.C. (vivien.casagrande@vanderbilt.edu) or G.P. (gopathy.purushothaman@vanderbilt.edu).

Received 5 March; accepted 6 April; published online 6 May 2012; doi:10.1038/nn.3106

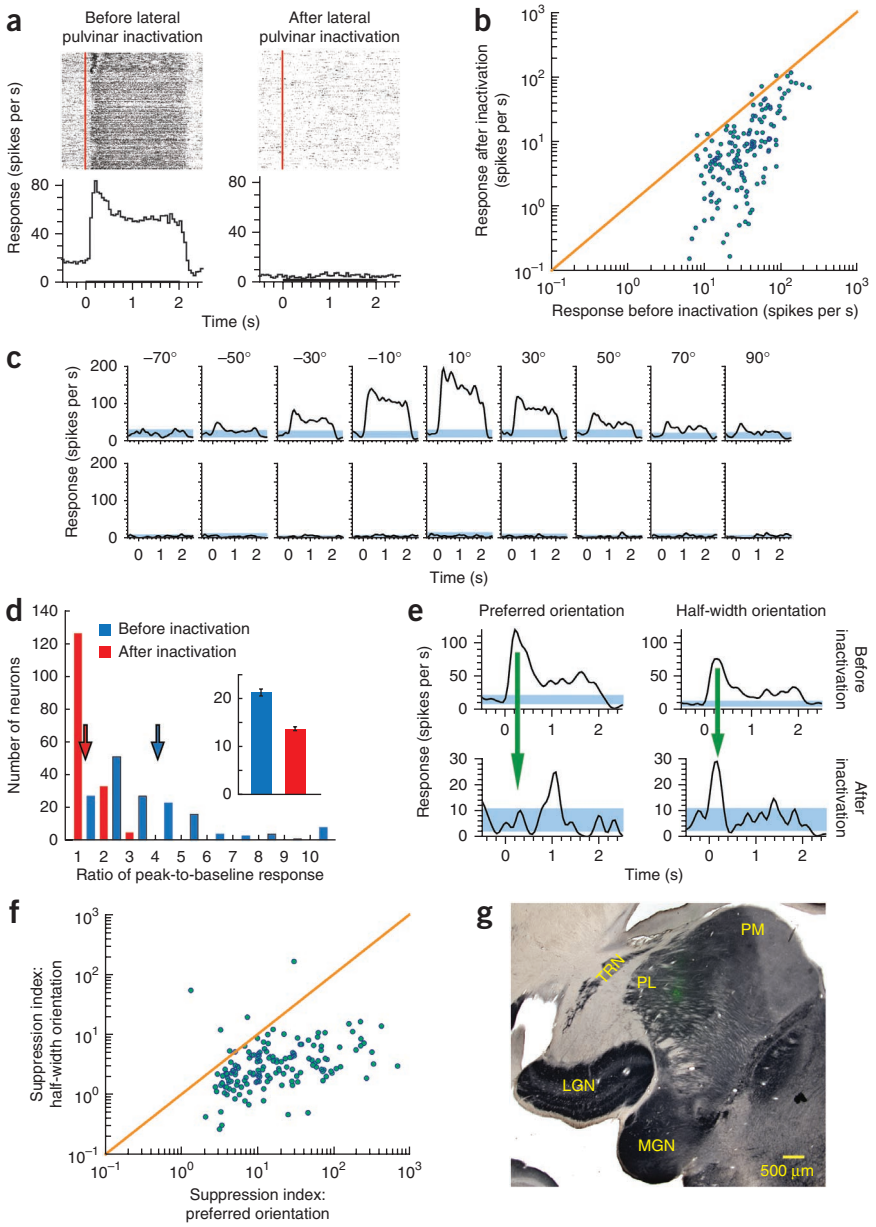

Figure 1 Reversibly inactivating lateral pulvinar almost abolishes visual responses in supra-granular layers of V1. (**a**) Raster plots representing each spike as a dot and PSTHs are shown for a sample neuron in layers 2–3 of V1 before (left) and after (right) lateral pulvinar inactivation. The red line on the raster plot shows visual input onset time and the black line on the abscissa of the PSTH shows the visual input presentation time. The responses that are shown are for a drifting sinusoidal grating presented in the neuron's receptive field at 18 different orientations. (**b**) Comparison of the average input-driven response before and after lateral pulvinar inactivation for all 164 V1 neurons. (**c**) PSTHs are shown separately for nine orientations at which this neuron was most responsive before lateral pulvinar inactivation. Blue bands represent 95% confidence interval around the mean baseline response measured before visual stimulation. (**d**) The phasic response, quantified as the ratio of peak-to-baseline activity, is shown for 164 V1 neurons before (blue) and after (red) lateral pulvinar inactivation. Arrows indicate the mean values of the distributions. Inset shows baseline responses. (**e**) PSTHs are shown for a layer 3 V1 neuron before (top) and after (bottom) lateral pulvinar inactivation for the preferred orientation (left) and half-width orientation (right). Responses are shown at different scales for the top and bottom rows. (**f**) Comparison of suppression indices at preferred and half-width orientations for all 164 V1 neurons. (**g**) A composite figure showing the injection in lateral pulvinar. A coronal section of the left thalamus was stained for cytochrome oxidase. A fluorescent image (green) was obtained with Alexa Fluor488–conjugated streptavidin as probe for the BDA mixed with the muscimol injected in lateral pulvinar. The fluorescence image was used to create a vector mask for the cytochrome oxidase image, thereby rendering transparent in the image all pixels with intensity above background in the fluorescent image. Fluorescence seen in the composite image is through these transparent pixels in the cytochrome oxidase image. Fluorescence was localized well in lateral pulvinar and was more than 1 mm away from the TRN and LGN. MGN, medial geniculate nucleus; PL, lateral pulvinar; PM, medial pulvinar; TRN, thalamic reticular nucleus.

within 6° of area centralis. We inactivated the lateral pulvinar neurons by infusing a small volume (0.5 µl) of the GABA agonist muscimol (Online Methods). We then repeated the V1 measurements. In 95% (156 of 164) of the V1 neurons that we studied in three animals, the characteristic visually driven responses were almost completely abolished after the visuotopically matched region of lateral pulvinar was inactivated (**Fig. 1a**,**b**). This change occurred at all orientations of the sinusoidal grating (**Fig. 1c**). The average visual response decreased from 43.1 ± 2.9 spikes per s (mean ± s.e.m.) to 15.45 ± 1.8 spikes per s (**Fig. 1b**), a significant change (Wilcoxon rank-sum test, $P = 0$, $n = 164$) of 64%. We quantified the visual responsiveness of V1 neurons by computing the ratio of post-stimulus peak response to the pre-stimulus baseline (or background) response. This ratio changed significantly as a consequence of lateral pulvinar inactivation (Wilcoxon rank-sum test, $P = 0$, $n = 164$), with the average value decreasing by 300% from 4.01 ± 0.24 (mean ± s.e.m.) to the near-baseline value of 1.34 ± 0.03 (**Fig. 1d**). Baseline V1 activity also changed significantly (Wilcoxon rank-sum test, $P < 0.001$, $n = 164$), decreasing by 36% after lateral pulvinar inactivation (**Fig. 1d**).

After lateral pulvinar injection, the phasic component of V1 response was suppressed more strongly near the original preferred orientation of the neuron than near nonpreferred orientations (**Fig. 1e**). We computed the suppression index as the divisive reduction in the ratio of the peak-to-baseline response that occurred with lateral pulvinar inactivation (Online Methods). Suppression at the preferred orientation (mean ± s.e.m. = 0.11 ± 0.01) was about fivefold stronger than at the half-width orientation (0.58 ± 0.10, Wilcoxon rank-sum test, $P < 10^{-30}$, $n = 164$; **Fig. 1f**).

Spatiotemporal extent of the lateral pulvinar injections

To exclude cases in which the injection in lateral pulvinar diffused into the LGN or the thalamic reticular nucleus (TRN), we mixed the injected muscimol with biotinylated dextran amine (BDA) and probed it with Alexa Fluor488–conjugated streptavidin (Online Methods).

In the three cases described above, complete reconstruction of the thalamus revealed that the fluorescence was confined to lateral pulvinar within 500 µm of the injection site, and no fluorescence was observed in either the LGN or the TRN (**Fig. 1g** and **Supplementary Figs. 3** and **4**). Slight effusion along the path of injection in one case was also confined to dorsal lateral pulvinar and did not encroach on the TRN (**Supplementary Fig. 4a**).

Strong binding to $GABA_A$ receptors and high-affinity uptake into GABAergic neurons and astrocytes keep injected muscimol locally sequestrated[30,31]. Studies with [^{3}H] muscimol have found that even for large 1-µl injections of muscimol, the region of effectiveness remains confined to about 1 mm over several hours[30,31]. The 500-µm regions of fluorescence that resulted from 0.5-µl injections in our cases are roughly consistent with these measurements. However, some studies that used large volume (up to 2 µl) muscimol injections have reported that behavioral deficits sometimes changed or strengthened 1–2 h after injection[32]. Effusion along the injection pipette or the slow spread of muscimol in the tissue at a rate of about 1–2 mm over 1–2 h could account for these observations[32] (see Online Methods). To test the latter possibility, we studied the temporal dynamics of the effect of lateral pulvinar injections by measuring V1 visual responses in 15-min intervals over several hours. These measurements showed that the average V1 visual response in the 15 min before the injection was 41.9 ± 6.1 spikes per s (mean ± s.e.m.). V1 visual responses started decreasing within a few minutes (<5 min) of the injection and the average response between 20 and 35 min after the lateral pulvinar injection was 10.4 ± 2.4 spikes per s (**Supplementary Fig. 5a**), a significant change (Wilcoxon rank-sum test, $P < 10^{-9}$, $n = 36$) of 75% from the pre-injection response. Notably, there was no significant change in V1 visual responses thereafter for up to 125 min after the injection (Wilcoxon rank-sum test, $P > 0.4$; **Supplementary Figs. 5b–d** and **6**). Because the LGN was 1.5–2.0 mm from the center of the injection at the closest approach in our cases (**Fig. 1g** and **Supplementary Figs. 3** and **4**), at the rate of diffusion implied by the above-mentioned behavioral studies (~1 mm h^{-1}), changes in V1 responses resulting from leakage into LGN could not have occurred sooner than 60–90 min after the injection. Thus, in addition to the histology, this analysis suggests that our results are consistent with the action of injected muscimol on proximal lateral pulvinar neurons rather than on the distant LGN neurons.

Our injections were made in the visuotopic region of lateral pulvinar that contained central receptive fields (**Fig. 1g** and **Supplementary Figs. 3** and **4**). The part of dorsomedial LGN closest to the center of these lateral pulvinar injections represents the lower visual field; more central LGN receptive fields are located posterolaterally further away from the center of these injections (**Supplementary Fig. 4**). Given that LGN and V1 receptive fields are retinotopically colocated, if the suppression of V1 responses were mainly a result of leakage of muscimol into LGN, then V1 receptive fields in the lower field must necessarily be affected for the more central receptive fields to be affected. In the three cases described above, the injection almost completely suppressed visual responses in central V1 receptive fields. However, the more eccentric a V1 receptive field was in the lower field, the more responsive it was to visual stimulation (**Supplementary Fig. 7**). This spatial gradient of the effect of the injection on V1 is also consistent with proximal action of muscimol on lateral pulvinar rather than its leakage into LGN.

LGN activity during inactivation of lateral pulvinar

To further ensure that LGN input to V1 was not accidentally disrupted by the lateral pulvinar injection, we performed two more direct controls. First, we injected a fluorophore-conjugated muscimol (FCM, Online Methods) into lateral pulvinar instead of the muscimol-BDA mixture. FCM is a single molecule in which the muscimol terminus

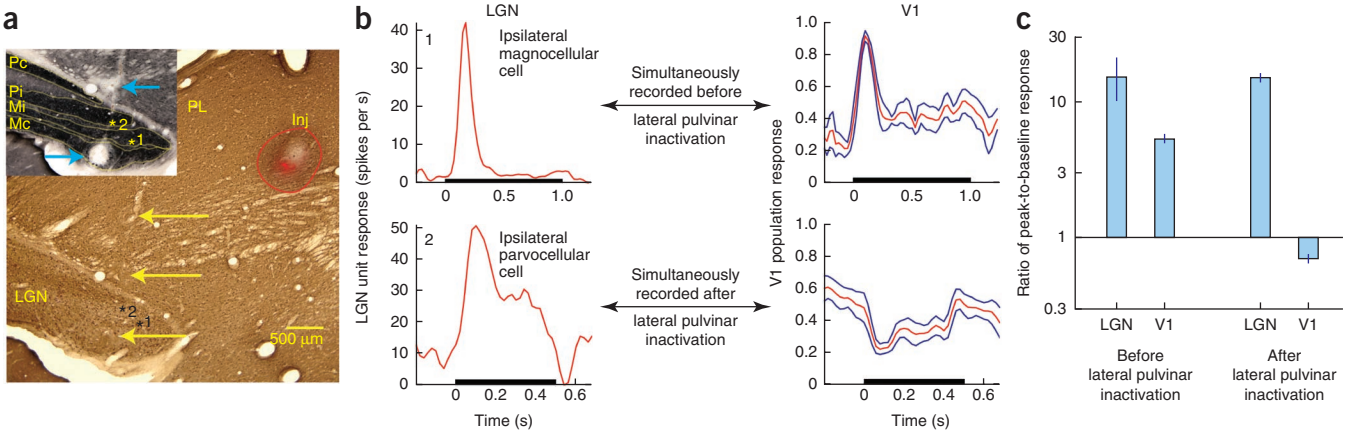

Figure 2 Gating of V1 output in the presence of LGN input. (**a**) Composite figure of the injection, created using the method mentioned above (**Fig. 1g**). Coronal section of left thalamus was stained for calbindin. Inj, injection in lateral pulvinar. Red fluorescence is from fluorophore-conjugated muscimol that was injected to inactivate this region of lateral pulvinar. The red outline shows the overall extent of the injection reconstructed from several successive sections through the thalamus. The region of inactivation is identical to the red fluorescent region, which is about 2 mm away from the LGN. The track from the electrode approaching LGN measurements sites is visible on the left. Yellow arrows mark three electrical lesions made along the electrode track for locating measurement sites in LGN. Inset shows the cytochrome oxidase–stained adjacent section with LGN layers marked and labeled. Blue arrows mark the two most ventral lesions. Numbers on the marked sites correspond to the numbers on the PSTHs shown in **b**. Pc, contralateral parvocellular layer; Pi, ipsilateral parvocellular layer; Mi, ipsilateral magnocellular layer; Mc, contralateral magnocellular layer. (**b**) PSTHs measured at two LGN sites are shown along with simultaneously measured V1 responses before (top) and after (bottom) lateral pulvinar inactivation. PSTH of a LGN neuron from the ipsilateral magnocellular layer in site 1 shows a brisk-onset transient response to a 1-s-long visual stimulation of its receptive field. The mean normalized PSTH of seven supra-granular V1 neurons, whose receptive fields completely overlapped that of the simultaneously measured LGN neuron (on the left), is shown in red. Blue lines indicate 1 s.e.m. Measurements at site 2 in the ipsilateral parvocellular layer were made after the lateral pulvinar injection. PSTH measured at this LGN site is shown along with the mean normalized PSTH of the simultaneously measured V1 responses. (**c**) Average ratio of peak-to-baseline response is shown for eight LGN and 52 V1 neurons before lateral pulvinar inactivation and 14 LGN and 84 V1 neurons after lateral pulvinar inactivation. Error bars indicate 1 s.e.m.

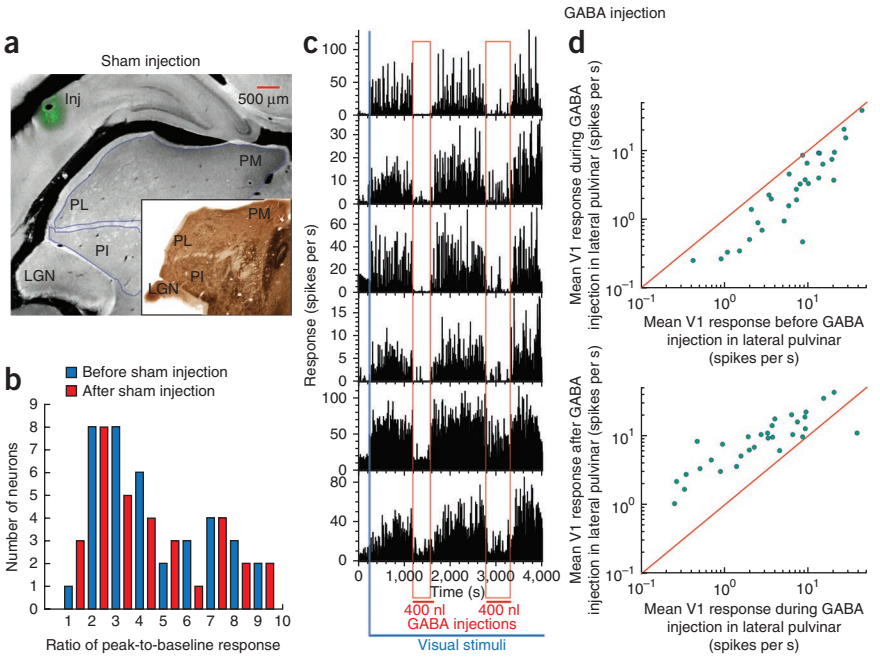

Figure 3 The process of lateral pulvinar injection does not compromise the integrity of V1 measurements. (**a**) Coronal section showing sham injection (Inj) above lateral pulvinar. Inset, adjacent section stained for acetylcholine esterase (AChE). (**b**) Ratio of peak-to-baseline response for 44 V1 neurons from layers 2–3 before (blue) and after (red) sham injection. (**c**) Effect of injecting in lateral pulvinar short-acting GABA on visually driven responses for layer 2–3 V1 neurons. The blue bar represents the beginning of presentation of the visual stimuli sequence consisting of a 1-s presentation of a drifting sinusoidal grating and a 1-s interstimulus interval. During this continuous visual stimulation of V1 neurons, two 400-nl injections of GABA were made in lateral pulvinar, about 1,500 s apart. The time period of each injection is shown marked by the vertical red band. (**d**) Comparisons of mean V1 responses during the pre-injection and peri-injection periods (top) and the mean V1 responses during the peri-injection and post-injection periods (bottom). PI, inferior pulvinar; PL, lateral pulvinar; PM, medial pulvinar.

binds to the GABA receptor and the BODIPY TMR-X terminus fluoresces near 572 nm, allowing us to determine the spatial extent of inactivation directly from the fluorescence (**Fig. 2a** and Online Methods).

Second, we monitored the integrity of LGN input to V1 by simultaneously measuring visual responses from LGN and V1 neurons both before and after the lateral pulvinar injection. To ensure that the measured LGN activity was largely responsible for the V1 activity assessed by the array, we selected LGN neurons with receptive fields completely overlapping those of the sampled V1 neurons[33]. One example is shown for measurements made before lateral pulvinar injection (**Fig. 2b**). Simultaneously measured responses for an ipsilateral magnocellular LGN neuron (**Fig. 2a**) and seven superficial layer V1 neurons (**Fig. 2b**), all of whose receptive fields were completely overlapping, were both brisk, with peak-to-baseline ratios of 18 and 3.68 ± 0.02, respectively. Another example is shown for measurements made after lateral pulvinar injection (**Fig. 2b**). The LGN response of this ipsilateral parvocellular neuron (**Fig. 2a**) was still brisk, with a peak-to-baseline ratio of 17, but the simultaneously measured V1 responses were suppressed, with a peak-to-baseline ratio of 0.46 ± 0.18 (**Fig. 2b**).

Several LGN sites were sampled both before and after the lateral pulvinar injection. For each site, responses of a LGN neuron were measured simultaneously with several V1 neurons whose receptive fields overlapped that of the LGN neuron. The peak-to-baseline ratio did not change significantly for LGN neurons after lateral pulvinar injection (Wilcoxon rank-sum test, $P > 0.39$; before lateral pulvinar injection, $n = 8$, mean ± s.e.m. = 15.31 ± 5.25; after lateral pulvinar injection, $n = 14$, 15.08 ± 0.02; **Fig. 2c**). For V1 neurons, the ratio changed significantly after lateral pulvinar injection (Wilcoxon rank-sum test, $P < 10^{-6}$; before lateral pulvinar injection, $n = 52$, mean ± s.e.m. = 5.32 ± 0.24; after lateral pulvinar injection, $n = 84$, 0.70 ± 0.04; **Fig. 2c**). These two controls showed that the integrity of LGN input to V1 was not compromised by the lateral pulvinar injection. The post-injection measurements included in the above analyses started 37 min after lateral pulvinar injection and finished 3 h later. Throughout this period, LGN was robustly responsive to visual stimulation.

Sham and GABA injections

To verify that the mechanics of making the injection did not compromise V1 measurements (for example, by displacing the electrode array during the insertion of the injectrode; see Online Methods), we performed two additional controls. First, although measuring the visual responses of V1 neurons with the array, we inserted the injectrode at the Horseley-Clarke coordinates for lateral pulvinar (Online Methods) and made a sham injection of the muscimol and BDA cocktail at a distance of 1.2 mm above the dorsal surface of lateral pulvinar (one animal; **Fig. 3a**). Peak-to-baseline ratios did not change significantly after the injection ($n = 44$, Wilcoxon rank-sum test, $P > 0.5$; **Fig. 3b**). This confirmed that the injection process did not adversely affect V1 measurements.

Second, we injected the fast and short-acting native inhibitory transmitter GABA into lateral pulvinar instead of the slow and long-acting $GABA_A$ receptor agonist muscimol. Each injection of 0.4 µl of GABA in lateral pulvinar resulted in an immediate and marked reduction of the visual responses of superficial layer V1 neurons (**Fig. 3c**). When injection was paused, stimulus-driven activity was immediately and fully restored in these neurons (**Fig. 3c**). We examined the responses of V1 neurons averaged in three distinct epochs: pre-injection (~200–1,200 s; **Fig. 3c**), peri-injection (~1,200–1,600 s; **Fig. 3c**) and post-injection (~1,600–2,800 s; **Fig. 3c**). Average response significantly changed (Wilcoxon rank-sum test, $P < 0.007$, $n = 31$) from the pre-injection period (10.2 ± 1.7 spikes per s) to the peri-injection period (5.4 ± 1.4 spikes per s), a decrease of 47% (**Fig. 3d**). Average response also significantly changed (Wilcoxon rank-sum test, $P < 10^{-4}$, $n = 31$) from the peri-injection period to the post-injection period (10.9 ± 1.7 spikes per s), an increase of 101% (**Fig. 3d**). This quick and complete recovery once again confirmed that the injection process did not compromise V1 measurements. The almost instantaneous effect that these small volume (400 nl) GABA injections had on V1 responses also fairly effectively ruled out leakage into LGN as the source of suppression of V1 responses. Histology confirmed that the injections were in lateral pulvinar and did not leak into LGN (**Supplementary Fig. 8**). In addition, this experiment also showed that injecting $GABA_A$ receptor ligands with different

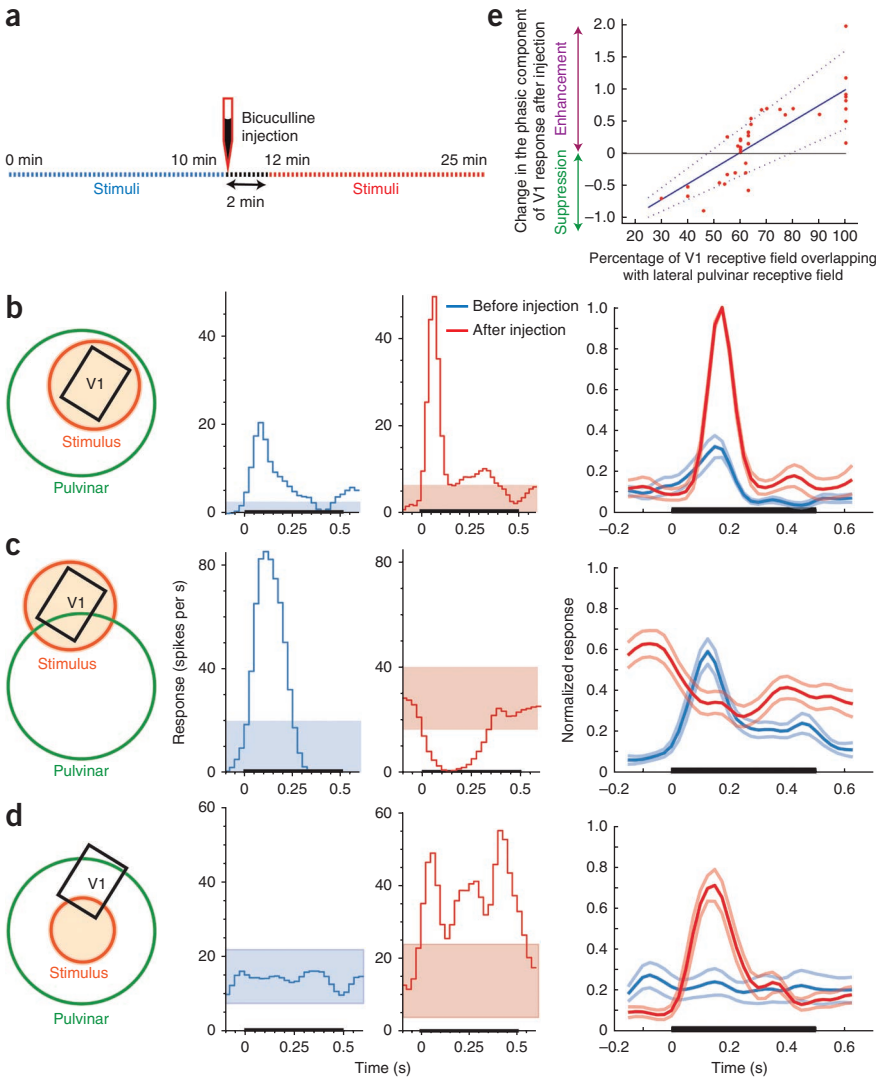

Figure 4 Exciting lateral pulvinar neurons responsive to a region boosts responses of V1 neurons to this region and suppresses responses to surrounding region. (**a**) Timing of response measurements and the injection of BMI. (**b**) In one subset of V1 neurons that we studied, V1 receptive fields (black) were enveloped by the injected lateral pulvinar receptive fields (green) and visual stimulation (orange) was centered on the V1 receptive fields. Visual responses of a V1 neuron with receptive field inside the excited lateral pulvinar receptive field are shown before (blue) and after (red) lateral pulvinar excitation. Colored bands represent 95% confidence interval about the baseline response. Right column shows the normalized responses of 14 V1 neurons in this subset, averaged over the pre-injection (thick blue line) and post-injection (thick red line) periods. Lighter lines represent 1 s.e.m. (**c**) In the second subset of V1 neurons that we studied, visual stimulation (orange) was centered about their receptive fields (black) that overlapped with the injected lateral pulvinar receptive fields by less than 60%. Brisk visual responses obtained before lateral pulvinar injection (blue) were suppressed after the injection (red). Right column shows the average PSTHs for the pre-injection (blue) and post-injection (red) periods. The average PSTH before lateral pulvinar injection in this case (right column, thick blue line) appears to be slightly larger than that seen in **b** as a result of normalization with respect to smaller post-injection responses. (**d**) In the third subset of V1 neurons, visual stimulation (orange) was centered about the lateral pulvinar receptive field and was marginal for the V1 receptive fields. V1 receptive fields were enveloped by the injected lateral pulvinar receptive fields. V1 neurons that hardly responded to the marginal stimulation of their receptive fields before lateral pulvinar injection (blue) showed a vigorous response after (red) the injection. (**e**) Change in the ratio of peak-to-baseline response is shown plotted on a logarithmic scale against the percentage of V1 receptive field overlapping with excited lateral pulvinar receptive fields. Regression result is shown as the continuous blue line and the dotted lines represent 95% confidence interval for the estimate of the regression slope.

molecular structures into lateral pulvinar obtained similar effects on V1 responses. Finally, these results are consistent with those of a previous study that reported reduction in V1 responses after injection of GABA into the lateral posterior (pulvinar) complex of the cat[34].

Effect of focal excitation of lateral pulvinar

We also measured visual responses in supra-granular V1 layers while focally exciting lateral pulvinar neurons (two animals). Drifting sinusoidal gratings were presented inside V1 receptive fields at the lower contrast of 14% (to reduce saturation effects) and at near-optimal orientations. To excite lateral pulvinar, we injected 0.4 µl of the $GABA_A$ receptor antagonist bicuculline methiodide (BMI). We compared V1 measurements from a 10-min interval before the injection with measurements from a 13–15-min interval after the injection (**Fig. 4a**). V1 receptive fields sampled by the array overlapped those of the injected lateral pulvinar neurons to varying extents. The baseline activity of all V1 neurons whose receptive fields were within 4–6° of the injected lateral pulvinar receptive fields changed significantly after injection (53 neurons from two animals, Wilcoxon rank-sum, $P < 0.008$), with an average increase of 72%.

For each V1 neuron, we normalized peristimulus time histograms (PSTHs) over the entire 25-min measurement period, including the pre- and post-injection intervals (**Fig. 4a**). Normalized PSTHs were then averaged across neurons for the pre- and post-injection periods separately. In V1 neurons whose receptive fields were fully enveloped by the injected lateral pulvinar receptive fields and were fully stimulated by the visual stimulus (**Fig. 4b**), the ratio of peak-to-baseline response changed significantly (Wilcoxon rank-sum, $P < 10^{-30}$, $n = 14$), increasing by 232% from 2.8 ± 0.40 to 9.3 ± 0.02 (**Fig. 4b**). V1 neurons whose receptive fields overlapped those of the injected lateral pulvinar neurons by less than ~60% showed a suppression of response as a consequence of the injection (**Fig. 4c**). The peak-to-baseline ratio changed significantly (Wilcoxon rank-sum, $P < 0.007$, $n = 22$; **Fig. 4c**), decreasing by 83% to 0.47 ± 0.01. In V1 neurons whose receptive fields were fully enveloped by the injected lateral pulvinar fields, but were only marginally stimulated by the visual stimulus that was centered on the lateral pulvinar receptive fields (**Fig. 4d**), the peak-to-baseline response changed significantly (Wilcoxon rank-sum, $P < 0.01$, $n = 17$), increasing by 483% from 1.2 ± 0.08 to 7.05 ± 0.60 (**Fig. 4d**). This latter group of V1 neurons behaved as if their receptive

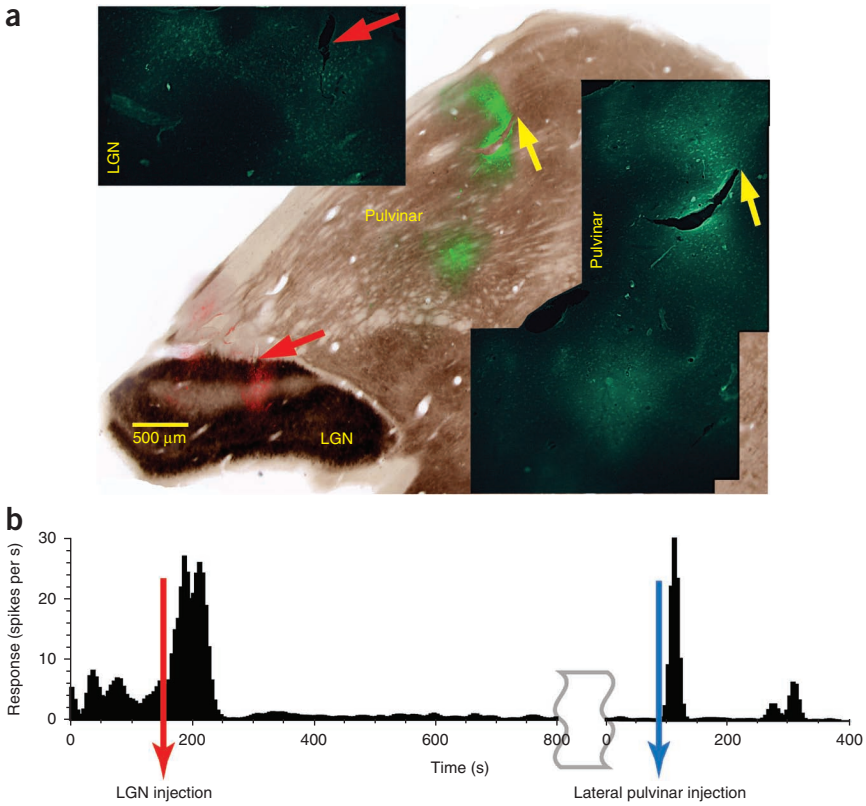

Figure 5 Kindling of V1 activity by lateral pulvinar excitation after LGN lesion. (**a**) Composite image showing the injections, created using the method mentioned above (**Fig. 1g**). Shown is a coronal section stained for AChE with ibotenic acid injections in false colors, green in lateral pulvinar and red in LGN. Insets show regions of injections stained with Fluoro-Jade C in higher magnification. Individual degenerating cells are seen labeled. (**b**) Changes in the baseline response of a supra-granular V1 neuron due to the injection of ibotenic acid in LGN and lateral pulvinar. The lateral pulvinar injection was made 30 min after the end of the timeline shown for the LGN injection.

fields had either enlarged or shifted toward the center of the injected lateral pulvinar receptive fields or both (**Fig. 4d**). For fully stimulated V1 receptive fields (**Fig. 4b**,**c**), a regression analysis revealed the effect of the receptive field overlap on the peak-to-baseline ratio to be significant (R^2 = 0.64, F = 66.5, P = 0, variance = 0.13; **Fig. 4e**). To classify V1 receptive fields unambiguously into these three qualitative categories (**Fig. 4b**–**d**), we selected only V1 neurons whose receptive fields were less than half the size of the injected lateral pulvinar receptive field for these *post hoc* analyses.

Histology showed that the BMI injections were localized in lateral pulvinar and did not diffuse into LGN (**Supplementary Fig. 9**). All three types of significant changes observed in V1 responses (**Fig. 4b**–**d**) occurred in minutes (~2 min) of small volume (400 nl) BMI injections in lateral pulvinar. This quick onset was consistent with the observed changes in V1 being a result of the action of injected material on proximal lateral pulvinar neurons rather than of leakage into distant LGN neurons. To further verify that leakage of the excitatory agent into LGN was not involved in kindling V1 neurons, we carried out a control in which we first injected the LGN and then the lateral pulvinar with ibotenic acid, a glutamate agonist, and observed the effect on neurons in the supra-granular layers of V1 (**Fig. 5a**). Baseline activity was continuously measured with an electrode array in layers 2–3 of V1. We injected a large 1.8-µl volume of ibotenic acid into all layers of LGN covering the region of visual space spanned by the receptive fields of V1 neurons sampled by the array. LGN excitation by ibotenic acid first produced an eightfold increase in V1 activity (Wilcoxon rank-sum, P = 0, n = 39; **Fig. 5b**). The excitotoxic apoptosis of LGN neurons that followed caused a significant change in V1 baseline activity (Wilcoxon rank-sum, $P < 10^{-30}$, n = 39), with an average decrease of 85%. After allowing 30–60 min for the apoptotic lesion of LGN to complete, we injected 1.0 µl of ibotenic acid into lateral pulvinar (**Fig. 5a**). Despite the significantly lower baseline activity, V1 neurons again showed a 14-fold increase in activity following this lateral pulvinar injection (Wilcoxon rank-sum, P = 0, n = 39; **Fig. 5b**). Fluoro-Jade C staining of degenerating neurons confirmed the location and extent of excitotoxic lesions in LGN and lateral pulvinar (**Fig. 5a** and Online Methods). These results fairly effectively rule out LGN's involvement in the excitatory kindling of V1 neurons and are consistent with findings that electrical stimulation of pulvinar elicits positive BOLD response in V1 of the macaque[35].

DISCUSSION

Our data indicate that removal of lateral pulvinar input can almost extinguish visual responses in the primary visual cortex and prevent the associated visual information from propagating beyond V1. The data also show that lateral pulvinar neurons can strongly boost V1 visual responses in the region of their receptive fields while suppressing responses to the surrounding region. These results suggest that the higher order thalamic nucleus pulvinar has a critical and integral part in the functioning of the visual cortex[36].

The spatial proximity of lateral pulvinar to LGN in the thalamus posed considerable technical challenges for us. Taken together, the extensive histological analyses of the injections (**Figs.1g** and **2a** and **Supplementary Figs. 3**, **4**, **8** and **9**), the temporal dynamics of changes in V1 responses following the injection of muscimol in lateral pulvinar (**Supplementary Figs. 5** and **6**), the spatial gradient of changes in visual responses across the central 6° of V1 following the injection of muscimol in lateral pulvinar (**Supplementary Fig. 7**), the use of fluorescent muscimol to directly determine the spatial extent of inactivation from fluorescence (**Supplementary Fig. 2a**), direct simultaneous measurement of LGN and V1 responses following lateral pulvinar injections (**Fig. 2b**,**c**), the almost instantaneous effects that small volume (400 nl) injections of GABA and BMI had on V1 responses, and the excitatory kindling of V1 from lateral pulvinar after LGN lesion all implicate the manipulation of neural activity in lateral pulvinar as the cause of the observed effects in V1. However, these experiments measured the net effect of manipulating lateral pulvinar activity on V1 and do not allow us to distinguish between the direct effect that lateral pulvinar exerts on V1 and the indirect effect exerted via pathways through higher visual cortex[4,36,37]. Nevertheless, our data reveal a powerful form of control that the pulvinar can exercise over information processed and propagated in the visual cortex. Overall, our results illustrate

a wide range of modulatory functions of a higher order thalamic nucleus in cortical information processing[36].

A role for lateral pulvinar in sustaining visual responses

How can lateral pulvinar effectively suppress geniculo-fugal visual input to V1? Quantitative accounting of our results requires more information, particularly about pulvinar afferents in V1 and the nature of lateral pulvinar's influence on V1 via the indirect pathway through extrastriate areas. However, some qualitative explanations can be suggested for how the direct pulvino-V1 circuit might be responsible for the observed effects. Several experimental and computational investigations have indicated that a balanced combination of inhibitory and excitatory inputs underlies cortical neural responses[38–43]. In this framework, our results could be accounted for if pulvinar provides potent excitatory synapses to V1. Many neurons in supra-granular layers that receive a disynaptic signal from the LGN will also receive a slightly delayed, quadrisynaptic geniculo-fugal signal via these lateral pulvinar synapses (**Supplementary Fig. 10**). Layer 5 cells in V1 that project to lateral pulvinar also receive input from supra-granular layers via their apical dendrites[44]. The resulting circuit may be lumped and depicted as consisting of a loop for computational purposes (**Supplementary Fig. 10**), although the system is clearly far more complex[36,45]. Under normal conditions, this pulvino-V1 loop might be necessary to drive and sustain the stimulus-evoked response. When lateral pulvinar is inactivated, the loss of the few, but potent, excitatory inputs from lateral pulvinar could result in a net inhibition that prevents visual responses from fully emerging. Stronger inhibition at the preferred orientation of the neuron, as postulated in some V1 models[42,43], would yield greater suppression of the visual response for the preferred orientation after lateral pulvinar inactivation.

A second possibility is that a gating signal from lateral pulvinar acts multiplicatively on the geniculo-fugal feedforward excitatory signal. Setting this lateral pulvinar gating signal low would suppress the geniculo-fugal excitatory input. These two possibilities are not mutually exclusive, as lateral pulvinar could gate feedforward excitatory inputs in a circuit with balanced net excitation and inhibition to the same effect. Thus, including lateral pulvinar inputs in current models of V1 circuitry and function might account for some of our results.

Pulvinar and control of bottom-up salience for attention

Lesion or chemical inactivation of pulvinar often results in deficits of visual attention[12–20,23,24]. Electrophysiological and imaging assays of pulvinar neural activity have also revealed links to visual attention[6,20,23–26]. Furthermore, pulvinar has reciprocal connections with both prefrontal and visual cortices[5]. These facts suggest a role for pulvinar in mediating visual attention, which requires coordinated control of top-down and bottom-up signal flows[46]. Specifically, pulvinar subnuclei interconnected with early visual areas could control stimulus-driven or bottom-up salience of visual responses in conjunction with goal-driven or top-down signals received via the subnuclei interconnected with pre-frontal and parietal areas[15,47,48].

A network model of visual attention has postulated that pulvinar controls and routes information in the window of attention up the visual cortical hierarchy by gating feedforward synapses[48]. Our data indicate that lateral pulvinar can control and gate V1 neural activity in a manner consistent with its hypothesized role in controlling bottom-up salience for selective attention. When the spatiotemporal context of a visual stimulus autonomously enhances its salience in conflict with behavioral or top-down goals, lateral pulvinar can suppress neural responses to this stimulus in early visual cortex (**Fig. 1**), thus biasing the competition in favor of behaviorally relevant stimuli[46]. When the window of attention is on a particular set of visual inputs, lateral pulvinar can boost neural responses to these inputs while simultaneously suppressing responses to surrounding inputs (**Fig. 4**), thus gating and routing attended signals up the cortical hierarchy[48]. This analogy between our results and models of visual attention has an important caveat. The large changes in activity observed in our experiments as a consequence of direct pharmacological manipulation of lateral pulvinar need not necessarily be commensurate with the magnitude of neural effects measured in behavioral experiments in which changes in activity are governed not only by engaging or disengaging attention, but also by other variables, such as attentional load, the spatiotemporal window of attention and fixational eye movements.

Behavioral consequences of pulvinar inactivation

We found strong suppression of V1 visual responses following the reversible inactivation of a retinotopic region of lateral pulvinar. There are important caveats in inferring the behavioral consequences of this result. Reversible inactivation or lesion of pulvinar in awake behaving animals and humans may or may not reveal a scotoma depending on many factors, including whether the affected region is restricted to parts of pulvinar that connect with early visual cortex or if it covers other subnuclei as well (for example, in the macaque ventro-lateral and centro-lateral, but not dorsomedial, part of the lateral pulvinar connect to areas V1 and V2)[5], whether the subject is fixating or free-viewing, whether viewing is binocular or monocular (if pulvinar inactivation/lesion is unilateral), the retinotopic size of the affected area relative to the range of allowed fixational eye movements, and whether measurements are made after possible reorganization[16–18]. Another critical issue in the emergence of a scotoma is the size of the affected region and the nature of the background against which it is assessed[49]. Lesions to subnuclei connected to higher cortical areas (for example, the dorsomedial part of lateral pulvinar[5]) are likely to have different types of behavioral consequences reflecting the functional properties of their projection zones[12–16,20]. Thus, although it is hard to predict what the behavioral consequences of our results might be, our data clearly show that higher order thalamic nuclei such as the pulvinar have a much more important role in the cortical processing of sensory information than was previously thought.

METHODS

Methods and any associated references are available in the online version of the paper.

Note: Supplementary information is available in the online version of the paper.

ACKNOWLEDGMENTS

We thank J. Mavity-Hudson for histology, S. Walston, Y. Jiang, D. Yampolsky, J. Mavity-Hudson, J. Patel and D. Rinker for help with experiments, D. Yampolsky for technical and computational assistance, and M. Feurtado for veterinary assistance. We thank F. Ebner, J. Kaas, R. Khumbani, J. Schall, P. Wallisch and K.-W. Yao for their suggestions and comments on the work. This work was supported by US National Institutes of Health grants R01-EY01778, P30-EY008126, T32-EY07135 and P30-HD15052.

AUTHOR CONTRIBUTIONS

G.P. and V.A.C. designed the experiments. G.P., R.M., K.L. and V.A.C. performed the experiments. G.P. analyzed the data and wrote the paper. G.P., R.M., K.L. and V.A.C. edited the manuscript. V.A.C. supervised the work.

COMPETING FINANCIAL INTERESTS

The authors declare no competing financial interests.

Published online at http://www.nature.com/doifinder/10.1038/nn.3106.
Reprints and permissions information is available online at http://www.nature.com/reprints/index.html.

1. Kandel, E.R., Schwartz, J.H. & Jessell, T.M. *Principles of Neural Science* (New York, McGraw-Hill, 2000).
2. Purves, D., Augustine, G.J. & Fitzpatrick, D. *Neurosciencez* (Sinauer Associates, 2004).
3. Van Essen, D.C., Anderson, C.H. & Felleman, D.J. Information processing in the primate visual system: an integrated systems perspective. *Science* **255**, 419–423 (1992).
4. Felleman, D.J. & Van Essen, D.C. Distributed hierarchical processing in primate cerebral cortex. *Cereb. Cortex* **1**, 1–47 (1991).
5. Kaas, J.H. & Lyon, D.C. Pulvinar contributions to the dorsal and ventral streams of visual processing in primates. *Brain Res. Rev.* **55**, 285–296 (2007).
6. Robinson, D.L. & Robinson, S.E. Pulvinar and visual salience. *Trends Neurosci.* **15**, 127–132 (1992).
7. Casanova, C. The visual functions of the pulvinar. in *The Visual Neurosciences* (eds. Werner, J.S. & Chalupa, L.M.) 592–608 (Cambridge, Massachusetts, MIT Press, 2004).
8. Benevento, L.A. & Rezak, M. The cortical projections of the inferior pulvinar and adjacent lateral pulvinar in the rhesus monkey (*Macaca mulatta*): an autoradiographic study. *Brain Res.* **108**, 1–24 (1976).
9. Rezak, M. & Benevento, L.A. A comparison of the projections of the dorsal lateral geniculate nucleus, the inferior pulvinar and adjacent lateral pulvinar to striate cortex (area 17) in the macaque monkey. *Brain Res.* **167**, 19–40 (1979).
10. Ogren, M.P. & Hendrickson, A.E. The distribution of pulvinar terminals in visual areas 17 and 18 of the monkey. *Brain Res.* **137**, 343–350 (1977).
11. Crick, F. & Koch, C. Constraints on cortical and thalamic projections: the no-strong-loops hypothesis. *Nature* **391**, 245–250 (1998).
12. Ward, R., Danziger, S., Owen, V. & Rafal, R. Deficits in spatial coding and feature binding following damage to the human pulvinar. *Nat. Neurosci.* **5**, 99–100 (2002).
13. Karnath, H.-O., Himmelbach, M. & Rorden, C. The subcortical anatomy of human spatial neglect: putamen, caudate nucleus, and pulvinar. *Brain* **125**, 350–360 (2002).
14. Arend, I. *et al.* The role of the human pulvinar in visual attention and action: evidences from temporal order judgment, saccade decision and anti-saccade tasks. *Prog. Brain Res.* **171**, 475–483 (2008).
15. Snow, J.C., Allen, H.A., Rafal, R.D. & Humphreys, G.W. Impaired attentional selection following lesions to human pulvinar: evidence for homology between human and monkey. *Proc. Natl. Acad. Sci. USA* **106**, 4054–4059 (2009).
16. Chalupa, L.M. A review of cat and monkey studies implicating the pulvinar in visual function. *Behav. Biol.* **20**, 149–167 (1977).
17. Ungerleider, L.G. & Christensen, C.A. Pulvinar lesions in monkeys produce abnormal scanning of a complex visual array. *Neuropsychologia* **17**, 493–501 (1979).
18. Bender, D.B. & Butter, C.M. Comparison of the effects of superior colliculus and pulvinar lesions on visual search and tachistoscopic pattern discrimination in monkeys. *Exp. Brain Res.* **69**, 140–154 (1987).
19. Rafal, R.D. & Posner, M.I. Deficits in human visual spatial attention following thalamic lesions. *Proc. Natl. Acad. Sci. USA* **84**, 7349–7353 (1987).
20. Wilke, M., Turchi, J., Smith, K., Mishkin, M. & Leopold, D.A. Pulvinar inactivation disrupts selection of movement plans. *J. Neurosci.* **30**, 8650–8659 (2010).
21. Fischer, J. & Whitney, D. Precise discrimination of object position in the human pulvinar. *Hum. Brain Mapp.* **30**, 101–111 (2009).
22. Smith, A.T., Cotton, P.L., Bruno, A. & Moutsiana, C. Dissociating vision and visual attention in the human pulvinar. *J. Neurophysiol.* **101**, 917–925 (2009).
23. Desimone, R., Wessinger, M., Thomas, L. & Schneider, W. Attentional control of visual perception: cortical and subcortical mechanisms. *Cold Spring Harb. Symp. Quant. Biol.* **55**, 963–971 (1990).
24. Petersen, S.E., Robinson, D.L. & Morris, J.D. Contributions of the pulvinar to visual spatial attention. *Neuropsychologia* **25**, 97–105 (1987).
25. Bender, D.B. & Youakim, M. The effect of attentive fixation in macaque thalamus and cortex. *J. Neurophysiol.* **85**, 219–234 (2001).
26. Kastner, S. *et al.* Functional imaging of the human lateral geniculate nucleus and pulvinar. *J. Neurophysiol.* **91**, 438–448 (2004).
27. Wilke, M., Mueller, K.M. & Leopold, D.A. Neural activity in the visual thalamus reflects perceptual suppression. *Proc. Natl. Acad. Sci. USA* **106**, 9465–9470 (2009).
28. Berman, R.A. & Wurtz, R.H. Signals conveyed in the pulvinar pathway from superior colliculus to cortical area MT. *J. Neurosci.* **31**, 373–384 (2011).
29. Ivanov, I. *et al.* Morphological abnormalities of the thalamus in youths with attention deficit hyperactivity disorder. *Am. J. Psychiatry* **167**, 397–408 (2010).
30. Mize, R.R. & White, D.A. [^{3}H]Muscimol labels neurons in both the superficial and deep layers of cat superior colliculus. *Neurosci. Lett.* **104**, 31–37 (1989).
31. Martin, J.H. Autoradiographic estimation of the extent of reversible inactivation produced by microinjection of lidocaine and muscimol in the rat. *Neurosci. Lett.* **127**, 160–164 (1991).
32. Hikosaka, O. & Wurtz, R.H. Modification of saccadic eye movements by GABA-related substances. II. Effects of muscimol in monkey substantia nigra pars reticulata. *J. Neurophysiol.* **53**, 292–308 (1985).
33. Reid, R.C. & Alonso, J.M. Specificity of monosynaptic connections from thalamus to visual cortex. *Nature* **378**, 281–284 (1995).
34. Molotchnikoff, S. & Shumikhina, S. The lateral posterior-pulvinar complex modulation of stimulus-dependent oscillations in the cat visual cortex. *Vision Res.* **36**, 2037–2046 (1996).
35. Logothetis, N.K. *et al.* The effects of electrical microstimulation on cortical signal propagation. *Nat. Neurosci.* **13**, 1283–1291 (2010).
36. Sherman, S.M. & Guillery, R.W. Distinct functions for direct and transthalamic corticocortical connections. *J. Neurophysiol.* **106**, 1068–1077 (2011).
37. De Pasquale, R. & Sherman, S.M. Synaptic properties of corticocortical connections between the primary and secondary visual cortical areas in the mouse. *J. Neurosci.* **31**, 16494–16506 (2011).
38. McCormick, D.A., Shu, Y.S. & Hasenstaub, A. Balanced recurrent excitation and inhibition in local cortical networks. in *Excitatory-Inhibitory Balance: Synapses, Circuits, Systems* (ed. Hensch, T.) 113–124 (Kluver Academic Press, New York, 2003).
39. Ferster, D. Orientation selectivity of synaptic potentials in neurons of cat primary visual cortex. *J. Neurosci.* **6**, 1284–1301 (1986).
40. Softky, W.R. & Koch, C. The highly irregular firing of cortical cells is inconsistent with temporal integration of random EPSPs. *J. Neurosci.* **13**, 334–350 (1993).
41. Borg-Graham, L.J., Monier, C. & Fregnac, Y. Visual input evokes transient and strong shunting inhibition in visual cortical neurons. *Nature* **393**, 369–373 (1998).
42. Somers, D.C., Nelson, S.B. & Sur, M. An emergent model of orientation selectivity in cat visual cortical simple cells. *J. Neurosci.* **15**, 5448–5465 (1995).
43. Mariño, J. *et al.* Invariant computations in local cortical networks with balanced excitation and inhibition. *Nat. Neurosci.* **8**, 194–201 (2005).
44. Callaway, E.M. Local circuits in primary visual cortex of the macaque monkey. *Annu. Rev. Neurosci.* **21**, 47–74 (1998).
45. Rockland, K.S. Convergence and branching patterns of round, type 2 corticopulvinar axons. *J. Comp. Neurol.* **390**, 515–536 (1998).
46. Desimone, R. & Duncan, J. Neural mechanisms of selective visual attention. *Annu. Rev. Neurosci.* **18**, 193–222 (1995).
47. Van Essen, D.C. Cortico-cortical and thalamo-cortical information flow in the primate visual system. in *Cortical Function: A View from the Thalamus* (eds. Casagrande, V.A., Guillery, R. & Sherman, M.) 173–185 (Elsevier, 2005).
48. Olshausen, B.A., Anderson, C.H. & Van Essen, D.C. A neurobiological model of visual attention and invariant pattern recognition based on dynamic routing of information. *J. Neurosci.* **13**, 4700–4719 (1993).
49. Ramachandran, V.S. & Gregory, R. Perceptual filling in of artificially induced scotomas in human vision. *Nature* **350**, 699–702 (1991).

ONLINE METHODS

Ten adult prosimian primates (*Otolemur garnettii*) of both sexes weighing 0.9–1.3 kg were used in these experiments according to approved protocols from the Institutional Animal Care and Use Committee at Vanderbilt University. Anesthesia was induced by an intraperitoneal injection of 30% urethane solution (1.25 g per kg of body weight) and maintained with 20% of induction dose every 2 h. Neuromuscular blockade was achieved with Vencuronium bromide (0.5–1.0 mg kg^{-1} h^{-1}). Animals respired room air via a ventilator, supplemented with O_2 as necessary, to maintain expired CO_2 at 4%. Pupils were dilated with 2% cyclopentolate (wt/vol) drops and contact lenses with sufficient power and 3-mm pupils were fitted to keep the monitor in clear focus on the retina.

Electrophysiology. V1 measurements were made using an electrode array. The dura was reflected and a Cyberkinetics 100 electrode array (Blackrock Microsystems) was pneumatically inserted over V1 and secured with 1% agarose in saline. Spikes were collected using a Bionics multichannel neural data acquisition system and sorted offline using Bayesian clustering methods (Plexon). LGN and pulvinar measurements were made with single electrodes using a 16-channel Plexon Multichannel Acquisition Processor. Simultaneous measurements in V1 and LGN were made using differential mode recordings on both multichannel systems with common reference. We included in the analyses every neuron whose stimulus-driven PSTH (before lateral pulvinar injection) deviated outside the 95% confidence interval about the mean baseline response (for the analyses following the BMI injections, an additional selection criterion based on receptive field size was used).

Receptive field mapping. To accurately map receptive fields, we used a modified version of Bishop's plotting table method[50]. Optic disks and retinal blood vessels were back reflected with a fiber-optic light source and plotted on a tangent screen 57 cm in front of the eyes. Area centralis was marked relative to the optical disk for each eye. Throughout the experiment, the positions of retinal landmarks were periodically checked for residual drifts of the paralyzed eyes. Stimuli such as moving lines, flashing lines and flashing spots were created using a projector with analog controls and backprojected onto the tangent screen. V1 receptive fields were then accurately hand mapped using these stimuli and plotted on the tangent screen along with retinal landmarks and the area centralis. Using a 45° mirror, the receptive fields, area centralis and retinal landmarks were then precisely transferred to a CRT monitor on which experimental stimuli were presented.

Visual stimuli. Visual stimuli were generated using a VSG 2/5 system (Cambridge Research) and presented on a 22-inch Sony CRT display at 120 Hz refresh rate. Sinusoidal gratings at the behaviorally optimal spatial (0.5 cycles per degree) and temporal frequency (2 Hz) were presented at orientations varying from 0° to 170° in steps of 10°. Each orientation, randomly selected, was presented for 1 s followed by a 1-s interstimulus interval during which the monitor was at the mean luminance of 12 cd m^{-2}. Gratings covered V1 receptive fields of interest and were presented at 50% contrast in lateral pulvinar inactivation experiments and at 14% contrast in experiments in which lateral pulvinar was excited. Simultaneous V1 and LGN measurements were made by finding an LGN neuron whose receptive field was completely inside V1 receptive fields of interest. A circular patch of light at high contrast (>90%) was flashed inside the LGN receptive field for 0.5–1 s followed by an equal duration interstimulus interval during which the monitor was at the mean luminance of 12 cd m^{-2}.

Injections. The central representation of LGN was first found using a single electrode, often by aiming for the posterior pole of the LGN at the Horsley-Clarke coordinates of anterior-posterior +3 and medial-lateral +7. Central representation in lateral pulvinar was then found by moving 1.5 mm more medial (see atlas of bush baby thalamus/pulvinar, http://www.psy.vanderbilt.edu/faculty/Casagrande/CasagrandeLab/BUSHBABYATLAS2.pdf). Receptive fields of lateral pulvinar neurons at this site were then accurately plotted. The electrode was replaced with a custom injectrode back-filled with the required cocktail. Previously mapped receptive fields were found again with the injectrode. The injectrode was then lowered by about 100 µm so that the tip of the pipette and not just the tip of the electrode reached the target. The injectrode was then pulled back by 100 µm and the cocktail was slowly infused. Pulling back the injectrode in this manner helps create a pocket in which the injected material stays confined, as indicated by dozens of cases of histology performed in our laboratory. Muscimol injections contained a 66.7 mM solution of muscimol (114 MW, Sigma-Aldrich) in a 1.6% solution of BDA (wt/vol, 10,000 MW, Invitrogen). GABA injections contained a 25 mM solution of GABA (103 MW, Sigma-Aldrich) in a 1.6% solution of BDA. Bicuculline injections contained a 5 mM solution of BMI (509 MW, Sigma-Aldrich) in a 1.6% solution of BDA. Fluorophore-conjugated muscimol injections contained 1 mg of muscimol, BODIPY TMR-X conjugate (Invitrogen) dissolved in 1 ml of 0.9% saline (wt/vol). Ibotenic acid injections contained a 5 mg ml^{-1} solution of ibotenic acid (158 MW, Sigma-Aldrich).

Histology. Animals were killed using sodium pentobarbital (Nembutal, 50–75 mg per kg). Animals were perfused through the heart with a saline rinse containing 0.05% sodium nitrite, followed by a fixative (2% paraformaldehyde (wt/vol) in 0.1 M phosphate buffer or 3% paraformaldehyde, 0.1% gluteraldehyde (wt/vol) and 0.2% saturated picric acid (vol/vol)) and a 10% sucrose solution (wt/vol). The brain was blocked coronally with a blade mounted at a known coordinate in a stereotax. The occipital cortex was removed and flattened between slides in 0.1 M phosphate buffer with 30% sucrose. Flattened pieces were frozen and tangentially sectioned. The surface vasculature was preserved in the first 100–150-µm section. The remaining tissue was sectioned at 52 µm. The thalamus was cut coronally. All sections were placed in 20% glycerol (vol/vol) in 0.1 M Tris-buffered saline (TBS) and frozen at −70 °C until staining. Cytochrome oxidase staining was used to confirm that the array was in the primary visual cortex (**Supplementary Fig. 2**). Cytochrome oxidase staining was performed by incubating sections in 0.2% DAB (D5636, Sigma), 0.3% cytochrome C (250600, Calbiochem), 0.15% catalase (C40, Sigma), 2% sucrose, 0.03% $CoCl_2$ (wt/vol) and 0.03% $NiNH_4SO_3$ (wt/vol) in 0.05 M phosphate buffer at 40 °C for 1–4 h until well differentiated. Tangential slices of the primary visual cortex stained for cytochrome oxidase were successively examined to confirm that the electrode tips were within layers 2–3 (**Supplementary Fig. 2**).

For AChE staining, we used a standard method[51]. Sections were pre-incubated in 0.1 M acetate buffer (pH 6.6), 0.1 M sodium citrate, 20 mM $CuSO_4$, 10^{-3} M tetraisopropylpyrophosphoramide and 5 mM $K_3Fe(CN)_6$ for 45 min. Sections were then incubated in a fresh solution as described above with the addition of 0.1% acetylthiocholine iodide (wt/vol) overnight, rinsed in 0.1 M phosphate buffer, mounted on gelatinized slides, defatted and coverslipped with a mixture of distyrene and xylene.

To visualize BDA injected in the cocktails, sections were rinsed three times in TBS, placed into 1:400 Alexa Fluor488–conjugated streptavidin (Invitrogen) in a buffer consisting of 0.1% sodium azide (wt/vol), 0.2% Triton X-100 (vol/vol) and 0.5% cold-water fish gelatin (vol/vol) for 2 h, rinsed once in the same buffer, and then twice in TBS. Sections were mounted and coverslipped with Vectashield (Vector).

For Fluoro-Jade C staining, sections were rinsed three times in TBS, mounted on subbed slides from distilled water (DH_2O), and placed on a 50 °C slide warmer for a minimum of 30 min. They were then placed into 80% ethanol and 1% sodium hydroxide (wt/vol) for 5 min, rinsed for 2 min in 70% ethanol, 2 min in DH_2O and then placed into 0.06% potassium permanganate (vol/vol) in DH_2O for 10 min. They were rinsed in DH_2O for 2 min and transferred into a solution of 0.0001% Fluoro-Jade C (Millipore) and 0.1% acetic acid (vol/vol) in DH_2O. Slides were rinsed three times in DH_2O, dried on the slide warmer for a minimum of 5 min, cleared in Citrisolve (Fisher) for 5 min and coverslipped.

Data analysis. PSTHs were computed by aligning responses to stimulus onset, binning spikes in 50-ms intervals and smoothing the binned averaged spike rate with a 150-ms-wide sliding Gaussian window. The ratio of peak-to-baseline response was estimated as the ratio of the post-stimulus peak of the PSTH to the pre-stimulus PSTH values averaged over the 500 ms before stimulus onset. Suppression index at an orientation was estimated as the ratio of the peak-to-baseline value before injection to its value after injection.

50. Bishop, P.O., Henry, G.H. & Smith, C.J. Binocular interaction fields of single units in the cat striate cortex. *J. Physiol.* **216**, 39–68 (1971).
51. Karnovsky, M.J. & Roots, L.A. 'direct coloring' thiocholine method for cholinesterases. *J. Histochem. Cytochem.* **12**, 219–221 (1964).